ARTICLE OPEN

Check for updates

Immediate and long-term effects of orbitofrontal cortex stimulation on EEG microstates in schizophrenia

Kexu Zhang[1,10], Qiang Hu[2,10], Yanli Zhang[3], Ningning Zeng[4], Min Wang[5], Kun Li[1], Ziliang Wang[3], Junfeng Sun[6]✉, Jijun Wang[7,8,9]✉ and Xiong Jiao[7]✉

Repetitive transcranial magnetic stimulation (rTMS) targeting the orbitofrontal cortex (OFC) has shown promise in treating schizophrenia, yet its immediate and long-term effects on brain dynamics remain unclear. This study investigated the electrophysiological impact of OFC-rTMS by analyzing EEG microstates in patients with schizophrenia and healthy controls. A total of 87 patients were randomized to receive either 20 sessions of 1 Hz OFC-rTMS or sham stimulation, while 51 healthy controls received a single active rTMS session. Resting-state EEG recordings were obtained at baseline, immediately after the first session, and following the full course of treatment. Microstate analysis was performed by clustering EEG topographies into four canonical classes and extracting temporal features. At baseline, patients exhibited elevated microstate C and reduced microstate D compared to controls. A single active session reduced microstate C occurrence in both groups, with no changes observed in the sham group. After 20 sessions, the active rTMS group showed a sustained decrease in microstate C and increased microstate D across multiple metrics. Notably, exploratory subgroup analysis revealed that clinical responders to OFC-rTMS exhibited greater immediate reductions in microstate C following the first session compared to non-responders. These findings suggest that OFC-rTMS induces both immediate and long-term modulation of EEG microstates in schizophrenia, particularly normalizing abnormalities in microstate C. Early EEG responses may serve as potential biomarkers for long-term therapeutic response.

Translational Psychiatry (2026)16:56 ; https://doi.org/10.1038/s41398-026-03810-3

INTRODUCTION

Schizophrenia is a severe mental illness marked by a combination of positive, negative, and cognitive symptoms that profoundly impair daily functioning. It continues to be one of the major causes of disability-adjusted life years (DALYs) attributed to mental disorders and a major worldwide health burden [1]. While antipsychotic medications remain the mainstay of treatment and are effective for many patients, approximately one-third show little or no response [2]. Moreover, these medications are frequently associated with considerable side effects [3], underscoring the urgent need for alternative and more tolerable therapeutic strategies.

Repetitive transcranial magnetic stimulation (rTMS) has emerged as a promising noninvasive neuromodulatory approach, offering the potential to modulate dysfunctional brain circuits without systemic side effects. Current clinical protocols—such as 10 Hz stimulation over the left dorsolateral prefrontal cortex (DLPFC) or 1 Hz over the left temporoparietal cortex—have shown efficacy in reducing certain symptom dimensions, particularly in negative symptoms and auditory verbal hallucinations [4]. However, treatment outcomes for schizophrenia remain inconsistent, and many patients fail to achieve meaningful improvement [5]. One potential limitation lies in the choice of stimulation target [6]. Given the heterogeneity of underlying circuit dysfunction in schizophrenia, exploring novel cortical targets may be essential for improving response rates and expanding the therapeutic potential of rTMS.

The orbitofrontal cortex (OFC), a prefrontal region involved in reward valuation, decision-making, and emotional regulation, has recently gained attention as a novel target for neuromodulation [7]. OFC dysfunction has been implicated in a range of psychiatric conditions, and rTMS targeting this region has shown promising results, particularly in depression [8, 9] and obsessive-compulsive disorder [10, 11]. However, the therapeutic potential of OFC-rTMS in schizophrenia has not been fully elucidated. Our earlier clinical study has already demonstrated its beneficial effects on negative symptoms and cognitive deficits [12]. Nevertheless, the underlying neurophysiological mechanisms remain unclear [13].

Electroencephalography (EEG) offers a noninvasive, cost-effective, and temporally precise method for capturing the rapid fluctuations of brain activity. Among EEG-based approaches, microstate analysis provides a unique framework for

[1]Department of Physical Therapy, Shandong Daizhuang Hospital, Jining, China. [2]Department of Psychiatry, Wuhu Hospital of Anding Hospital (The Fourth People's Hospital of Wuhu), Wuhu, Anhui, China. [3]Department of Psychiatry, Zhenjiang Mental Health Center, Zhenjiang, China. [4]Cognitive Neuroscience Center, University Medical Center Groningen, Groningen, Netherlands. [5]Department of Psychology, School of humanities and social sciences, University of Science and Technology of China, Hefei, China. [6]Shanghai Med-X Engineering Research Center, School of Biomedical Engineering, Shanghai JiaoTong University, 200030 Shanghai, China. [7]Shanghai Key Laboratory of Psychotic Disorders, Shanghai Mental Health Center, Shanghai JiaoTong University School of Medicine, 200030 Shanghai, China. [8]CAS Center for Excellence in Brain Science and Intelligence Technology (CEBSIT), Chinese Academy of Science, Shanghai 200031, China. [9]Nantong Fourth People's Hospital&Nantong Brain Hospital, Nantong, Jiangsu 226000, China. [10]These authors contributed equally: Kexu Zhang, Qiang Hu. ✉email: jfsun@sjtu.edu.cn; jijunwang27@163.com; jiaoxiong@sjtu.edu.cn

Received: 17 September 2025 Revised: 12 December 2025 Accepted: 15 January 2026
Published online: 23 January 2026

characterizing global brain dynamics by segmenting spontaneous neural activity into brief, quasi-stable topographic patterns, typically lasting 60 to 120 milliseconds [14]. These microstates are thought to reflect the transient activation of large-scale functional brain networks and thus offer a dynamic marker of brain organization [15]. Four canonical microstates—A through D—have been consistently identified across developmental stages and clinical populations [16]. Prior studies have linked microstate A to the auditory system, B to visual processing, C to the salience network, and D to attentional control [17]. In schizophrenia, alterations in EEG microstates have emerged as robust and consistently observed features. Meta-analyses summarizing the existing literature have reported an increase in microstate C, alongside reductions in microstate D, across diverse cohorts [18, 19]. Cross-sectional comparisons across healthy individuals, clinical high-risk populations, and patients at different stages of schizophrenia suggest that these alterations worsen with disease progression [20–22]. These findings support the utility of microstate features as state-sensitive indicators of schizophrenia disorder. Beyond its diagnostic relevance, microstate analysis has also been applied to evaluate the effects of rTMS in various conditions such as disorders of consciousness [23], depression [24], addiction [25], and Parkinson's disease [26], demonstrating its sensitivity to stimulation-induced changes. Applying microstate analysis to OFC-rTMS may offer mechanistic insight into how neuromodulation alters large-scale brain dynamics in schizophrenia.

In this study, we used EEG microstate analysis to investigate the impact of OFC-rTMS on large-scale brain dynamics in schizophrenia. To capture both immediate and long-term effects of stimulation, we assessed microstate parameter changes following a single session of OFC-rTMS in patients and healthy controls, as well as after a 20-session treatment intervention in patients. Based on established alterations in microstates C and D in schizophrenia, we hypothesized that OFC-rTMS would reduce abnormal salience-related activity (microstate C) and enhance attentional network dynamics (microstate D), reflecting normalization of functional brain states associated with symptom improvement.

METHOD

Participants

Using the inclusion and exclusion criteria shown in Figure S1, 98 individuals with first episode schizophrenia (FES) were recruited from the First Psychiatric Hospital of Harbin, Heilongjiang Province, China. All patients met Diagnostic and Statistical Manual of Mental Disorders, Fifth Edition (DSM-5) diagnostic criteria for schizophrenia, confirmed independently by two board certified psychiatrists through structured clinical interviews. Furthermore, 51 healthy controls (HC) who were matched for age and sex and had no prior history of neurological or mental disorders were enrolled. Prior to their involvement, each subject gave written informed consent. The study was carried out in compliance with the Declaration of Helsinki, approved by the First Psychiatric Hospital of Harbin's Ethics Committee (IRB2019-004), and registered in the Chinese Clinical Trial Registry (ChiCTR2000041106).

The randomized controlled trial procedure is illustrated in Figure S1. Upon enrollment, each participant was assigned a random number generated by computer, and based on this number was allocated to either the rTMS group (N = 53) or the sham group (N = 45). The sample size was calculated to achieve a statistical power of approximately 83% at a significance level of 0.05 to detect the expected effect on PANSS scores (medium effect size, Cohen's f = 0.15). Following allocation, each participant underwent a 20-day intervention. During the trial, 7 participants in the rTMS group and 3 in the sham group dropped out due to inability to complete EEG acquisition, clinical assessments, or voluntary withdrawal. One additional participant in the rTMS group was excluded due to excessive EEG noise. The final analysis included 45 participants in the rTMS group, 42 in the sham group, and 51 in the HC group. Table S1 provides a summary of the three groups' clinical and demographic information. Age and sex did not differ significantly amongst the three groups (HC, rTMS, and sham). Years of education differed significantly across groups ($F(2, 135) = 5.157$, $p = 0.007$, $\eta^2_p = 0.168$), primarily reflecting differences between patients and healthy controls ($T(136) = 2.899$, $p = 0.004$, Cohen's $d = 0.511$), while no significant difference was found between the rTMS and sham groups.

Intervention

All patients received one rTMS session per day for 20 consecutive days. The rTMS group received low-frequency (1 Hz) rTMS targeting the right OFC, while the sham group underwent the same procedure using an inverted coil (rotated 180°) to prevent effective stimulation. The stimulation target was localized according to the international 10-10 EEG system, corresponding to the AF8 electrode position [8, 9]. A MagPro R30 stimulator (MagVenture, Denmark) with a 120° angled figure-eight coil (Cool D-B80) was used to deliver the stimulation. Each session included 12 stimulation trains lasting 60 seconds each, separated by 30-second inter-train intervals, for a total duration of 17.5 min and 720 pulses per session. Before the TMS experiment, the resting motor threshold (RMT) was determined by administering single pulses across the left primary motor cortex and finding the minimum intensity required to elicit motor-evoked potentials of ≥50 μV in amplitude in at least 50% of trials. The rTMS intensity was set at 110% RMT. Similar stimulation parameters have been applied in previous clinical neuromodulation studies and have demonstrated acceptable safety and therapeutic potential in psychiatric populations [8, 9, 27]. Blinding was implemented at the participant and outcome assessor levels. Patients were unaware of their treatment allocation, and symptom ratings were conducted by trained clinicians blinded to group assignment. Intervention operators necessarily knew the group allocation to correctly administer the stimulation. However, they did not participate in clinical assessments or data analysis.

Pharmacological therapy was also administered during the intervention period. In the rTMS group, 37 patients were treated with olanzapine and 8 with aripiprazole, while in the sham group, 35 and 7 patients received these medications, respectively. The prescribed antipsychotic dosage typically fell within the range of 10 to 15 mg per day.

Clinical Assessment and EEG Acquisition

The timeline of clinical assessments and EEG recordings is illustrated in Figure S2A. Clinical assessments were conducted at baseline and after the 20-day intervention. Symptom severity was evaluated using the Positive and Negative Syndrome Scale (PANSS) and the Clinical Global Impression scale (CGI), with PANSS serving as the primary outcome measure for assessing treatment-related improvements in patients with schizophrenia.

Resting-state EEG recordings were obtained from both schizophrenia patients and healthy controls. Healthy participants received a single session of OFC-rTMS and underwent EEG recordings before and after stimulation. Patients completed EEG at three time points: baseline (before the first session), acute (immediately after the first session), and post-treatment on day 21 (the day after completing the 20-day intervention). To avoid external interference, the recordings were conducted in a sound-attenuated, electrically shielded room. During each session, participants sat comfortably with their eyes closed and were instructed to remain relaxed but awake. EEG data were collected using a 64-channel system (Brain Products GmbH, Germany). The reference electrode was placed on the nose, and AFz served as the ground. Electrode impedances were kept below 5 kΩ throughout all recordings. Each session lasted for 5 min, with a continuous sampling rate of 1000 Hz. All recordings were visually inspected for quality, and care was taken to ensure consistent recording conditions across sessions and participants.

EEG data analysis

All EEG data were preprocessed and analyzed using EEGLAB (version 2022) [28] and custom scripts in MATLAB R2022b. Preprocessing began with automatic detection and rejection of bad channels, followed by spherical spline interpolation to ensure a consistent 64-channel configuration. The data were then bandpass filtered between 0.1 and 40 Hz and notch filtered from 49 to 51 Hz to eliminate line noise. Continuous EEG recordings were segmented into 10-second non-overlapping epochs, and any epochs containing amplitudes exceeding ±100 μV were excluded. Independent Component Analysis (ICA) was then used to detect and remove common artifacts, including eye movements, muscle activity, and cardiac signals. Finally, the data were re-referenced to the common average to improve spatial consistency across electrodes.

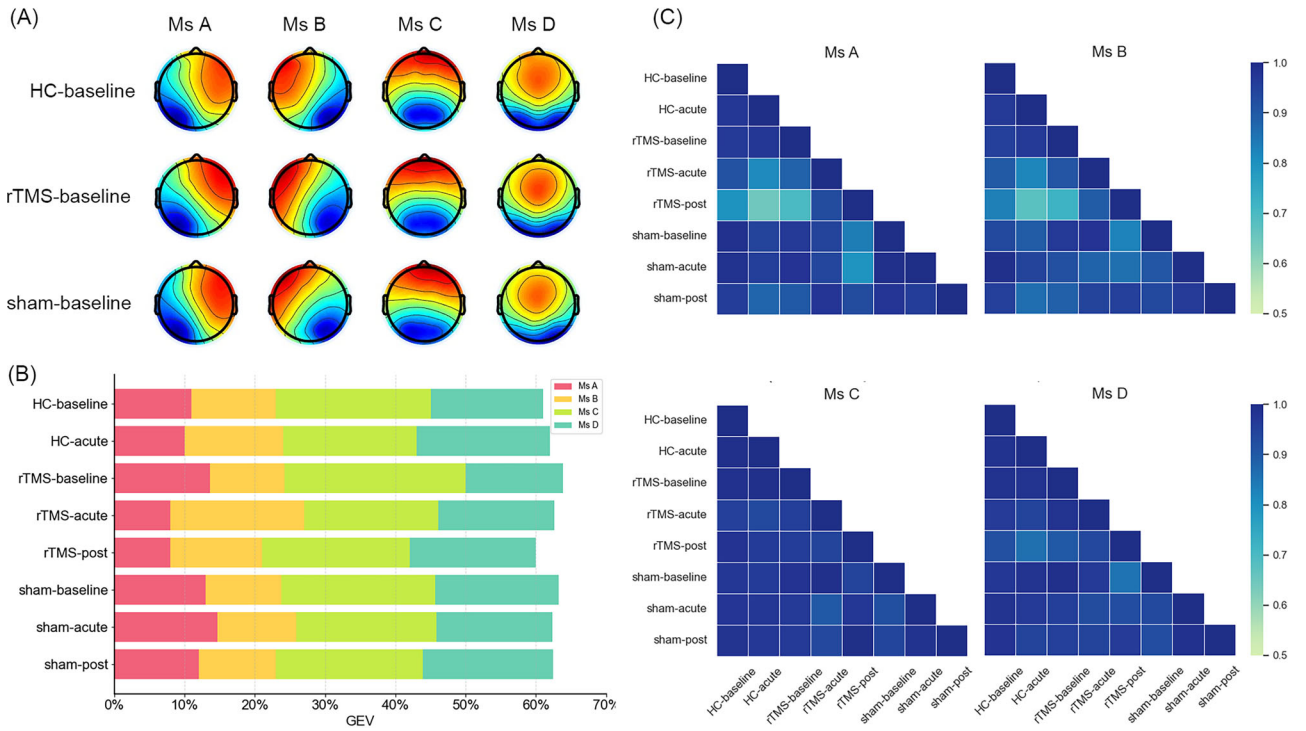

Fig. 1 Microstate clustering results. A Group-level microstate topographies at baseline in the HC, rTMS, and sham groups, labeled into four classes (A–D); (**B**) Global explained variance (GEV) of the four-cluster topographies across groups and conditions; (**C**) Spatial correlation coefficients between corresponding microstate maps across groups and conditions. MS, Microstate.

Microstate analysis was conducted following the workflow illustrated in Figure S2B. Global Field Power (GFP) was computed at each time point as the standard deviation across all electrodes, and only topographies at GFP local maxima were retained for clustering, as they represent the most stable spatial configurations [29]. A modified k-means clustering algorithm was used for microstate segmentation [30]. First, the optimal number of clusters was determined by applying the Krzanowski–Lai (KL) criterion to the entire dataset pooled across all participants and conditions [16]. Clustering was then performed separately within each group and condition to obtain initial microstate maps. The spatial consistency of these maps was assessed using pairwise spatial correlations across groups. Finally, the microstate templates derived from the healthy control group at baseline were selected as the reference maps, and all individual datasets were back-fitted to these templates for parameter extraction. The resulting microstate templates were subsequently back-fitted to the continuous EEG data. Specifically, for each GFP peak, the microstate category was assigned based on the template exhibiting the highest spatial similarity, quantified by the Pearson correlation coefficient between the template and the EEG topography at that peak. For time points between GFP peaks, the microstate label was propagated from the nearest GFP peak, ensuring that every time point in the EEG signal was assigned to one of the identified microstate classes. This procedure follows standard microstate analysis methods [31]. From the resulting microstate sequences, temporal features were extracted, including duration (mean time a microstate remains stable), coverage (percentage of total recording time occupied), and occurrence (mean number of appearances per second). Additionally, transition probabilities, defined as the likelihood of switching from one specific microstate to another, were calculated to capture the dynamic characteristics of state transitions.

Statistical analysis

All statistical analyses were carried out using Jamovi (version 2.3). The Shapiro-Wilk test was used to assess data normality, and Levene's test was applied to examine the homogeneity of variances. Depending on the distribution, comparisons between two independent groups were conducted using independent-samples t-tests or Mann-Whitney U tests, while paired t-tests or Wilcoxon signed-rank tests were applied for within-subject comparisons. For categorical variables, chi-square tests were applied. To assess changes over time and differences between groups, repeated-measures ANOVA was performed on clinical symptom scores and EEG microstate parameters. To control for multiple comparisons, false discovery rate (FDR) correction was used, with significance set at FDR-adjusted $q < 0.05$.

To assess the clinical efficacy of OFC-targeted rTMS in schizophrenia, changes in PANSS scores from baseline to after the 20-session intervention were compared between the rTMS and sham groups. To assess the effects of OFC-rTMS on brain dynamics, microstate parameters were analyzed in three contexts: (1) immediate effects in healthy controls after a single session (baseline vs. acute), (2) immediate effects in schizophrenia patients after the first session (baseline vs. acute), and (3) long-term effects in patients after the full intervention (baseline vs. post-treatment).

RESULT

At baseline, the rTMS and sham groups were comparable in symptom severity, as measured by the PANSS and CGI scores. Following the 4-week intervention, a significant time × group interaction in PANSS scores ($F(1, 85) = 17.104$, $p < 0.001$, $\eta^2_p = 0.168$) indicated differential symptom changes over time. Post hoc analyses revealed that the rTMS group showed a significantly greater reduction in PANSS scores compared to the sham group (rTMS group: -23.58 ± 9.83, sham group: -13.83 ± 12.08; $T(85) = 4.139$, $p < 0.001$, Cohen's $d = 0.888$), supporting the therapeutic efficacy of OFC-targeted rTMS in reducing schizophrenia symptoms in our previous study [12].

Microstate clustering results and baseline comparison

Based on the KL criterion applied to the entire dataset, four microstate classes were identified as the optimal number for clustering. Accordingly, for each group and each recording condition (baseline, acute, and post-treatment), EEG data were separately clustered into four microstates. The resulting topographic maps were labeled A through D based on their spatial configuration, and the group-level baseline maps are illustrated in Fig. 1A. The global explained variance (GEV) of the clustering solution exceeded 60% in all groups and conditions (Fig. 1B).

Spatial correlation coefficients between corresponding microstate classes across groups and conditions ranged from 0.72 to 0.99 (Fig. 1C). To control for spatial variability in template maps, all subsequent temporal parameter and transition probability analyses were performed using a back-fitting procedure based on the baseline HC group's microstate templates. Additionally, to account for inter-individual variability, for each participant and each microstate class, the average topography of all time points labeled as that microstate was computed and then correlated with the corresponding baseline HC template. The range of these correlations across groups was as follows: A, 0.598-0.690; B, 0.617-0.673; C, 0.610-0.772; D, 0.615-0.788. The relatively lower correlations are attributable to the inclusion of time points with lower signal-to-noise ratio. One-way ANOVA for each microstate showed no significant group differences (all $p \geq 0.078$), indicating that inter-individual variability did not produce systematic deviations in the topographies.

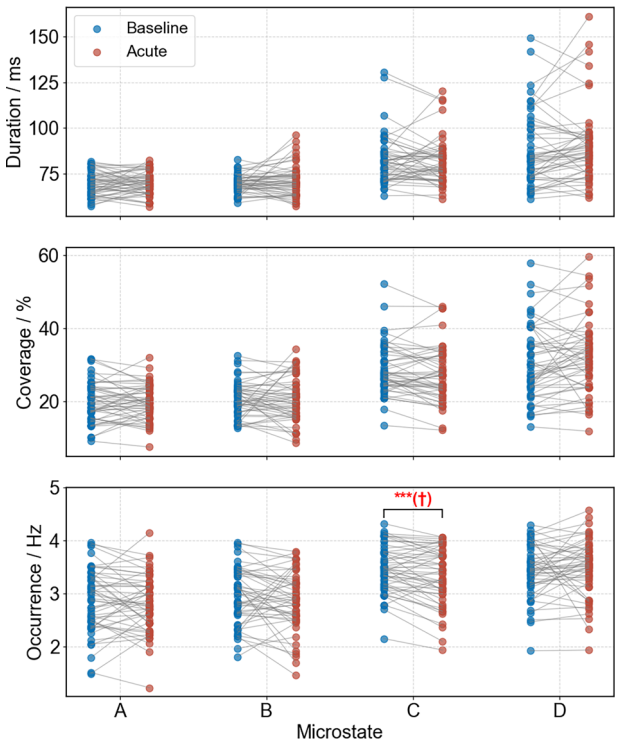

Fig. 2 Immediate effects of OFC-rTMS on microstate parameters in healthy controls. Within-group comparisons show changes in the duration, coverage, and occurrence of microstates A–D before and after a single session of OFC-rTMS. *p < 0.05, **p < 0.005, ***p < 0.001, †q < 0.05.

Baseline comparisons of microstate temporal parameters between patients with FES and HC are presented in Figure S3. Since years of education differed between patients and healthy controls, group comparisons were performed using ANCOVA with education included as a covariate. Compared to the HC group, the patients group exhibited significantly increased coverage ($F(1133) = 9.727$, $p = 0.002$, FDR-corrected $q = 0.024$, $\eta^2_p = 0.068$) and occurrence ($F(1133) = 18.433$, $p < 0.001$, FDR-corrected $q = 0.002$, $\eta^2_p = 0.122$) of microstate C, along with decreased duration of microstate D ($F(1133) = 9.541$, $p = 0.002$, FDR-corrected $q = 0.024$, $\eta^2_p = 0.067$). Transition probability analysis revealed that the FES group showed significantly increased probabilities of transitioning from microstates A ($F(1133) = 8.842$, $p = 0.003$, FDR-corrected $q = 0.024$, $\eta^2_p = 0.062$), B ($F(1133) = 4.181$, $p = 0.043$, $\eta^2_p = 0.030$), and D ($F(1133) = 5.007$, $p = 0.027$, $\eta^2_p = 0.036$) to microstate C, relative to the HC group (Figure S4).

Immediate effects of single-session OFC-rTMS on microstate dynamics

Figure 2 illustrates changes in microstate temporal parameters in the HC group following a single session of OFC-rTMS. A significant reduction was observed in the occurrence of microstate C ($T(50) = 3.223$, $p = 0.002$, FDR-corrected $q = 0.048$, Cohen's $d = 0.451$). Transition probability analysis further revealed a decreased likelihood of transitions from microstate A to C ($T(50) = 2.175$, $p = 0.034$, Cohen's $d = 0.305$) and an increased likelihood of transitions from A to D ($T(50) = 2.054$, $p = 0.045$, Cohen's $d = 0.288$), as shown in Supplementary Figure S5.

Figure 3 summarizes the effects of single-session active or sham OFC-rTMS on microstate temporal characteristics in patients with schizophrenia. For microstate C, a significant time × group interaction was found for coverage ($F(1, 85) = 6.031$, $p = 0.016$,

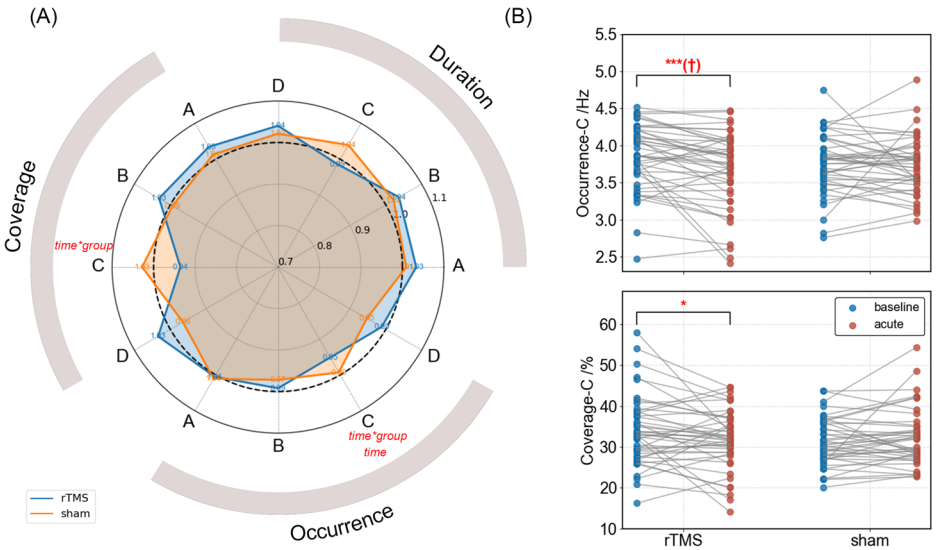

Fig. 3 Immediate effects of OFC-rTMS on EEG microstate parameters in patients with schizophrenia. A Ratio (post/pre) of duration, coverage, and occurrence for microstates A–D in the rTMS and sham groups following a single stimulation session. Significant effects identified by repeated-measures ANOVA are indicated. **B** Post hoc within-group comparisons for microstate parameters showing significant time × group interactions. *p < 0.05, **p < 0.005, ***p < 0.001, †q < 0.05.

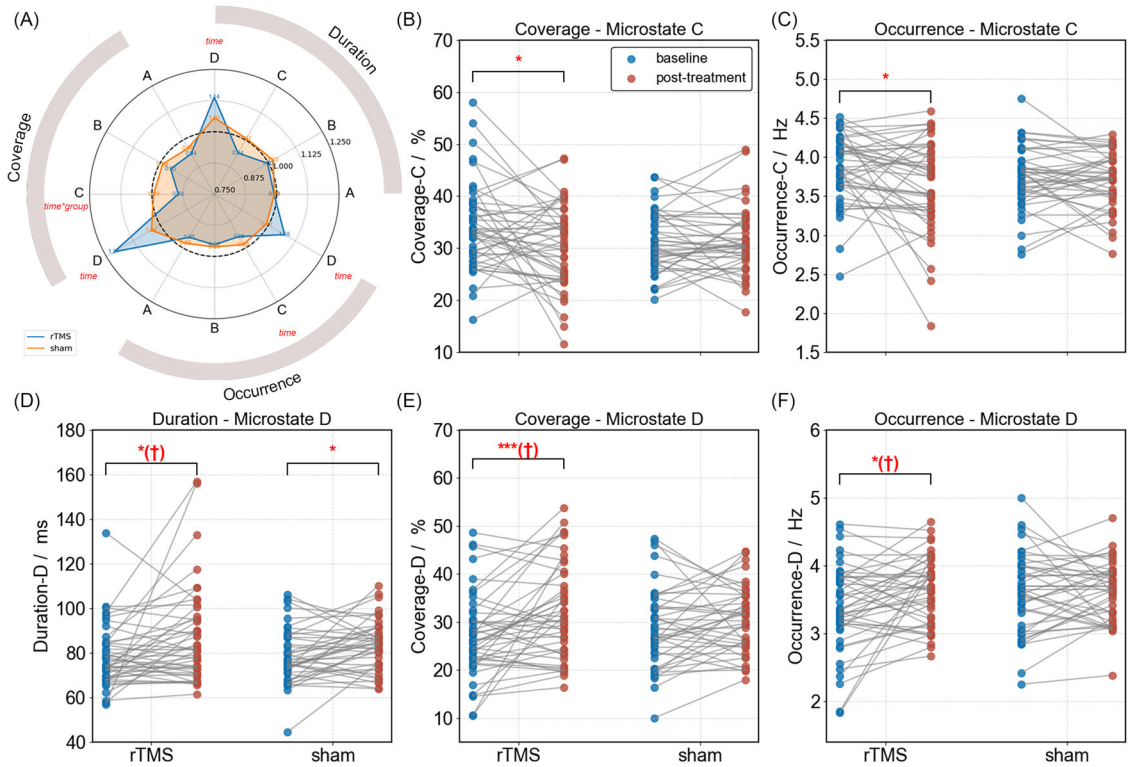

Fig. 4 Long-term effects of OFC-rTMS on EEG microstate parameters in patients with schizophrenia. A Ratio (post/pre) of duration, coverage, and occurrence for microstates A–D in the rTMS and sham groups following the intervention. Significant effects identified by repeated-measures ANOVA are indicated. **B–F** Post hoc within-group comparisons for microstate parameters showing significant time effects or time × group interactions. *p < 0.05, **p < 0.005, ***p < 0.001, †q < 0.05.

$\eta^2_p = 0.065$), while occurrence showed both a significant main effect of time ($F(1, 85) = 6.870$, $p = 0.010$, $\eta^2_p = 0.075$) and a time × group interaction ($F(1, 85) = 4.840$, $p = 0.030$, $\eta^2_p = 0.049$). Post hoc analyses revealed that the rTMS group showed significant reductions in both coverage ($T(44) = 2.111$, $p = 0.040$, Cohen's $d = 0.315$) and occurrence ($T(44) = 3.595$, $p < 0.001$, FDR-corrected $q = 0.019$, Cohen's $d = 0.536$) of microstate C, whereas no significant changes were observed in the sham group (all $p > 0.263$). In terms of state transition dynamics, significant time × group interactions were observed for transitions from microstate A to C ($F(1, 85) = 10.000$, $p = 0.002$, FDR-corrected $q = 0.048$, $\eta^2_p = 0.105$) and from B to C ($F(1, 85) = 4.310$, $p = 0.041$, $\eta^2_p = 0.052$). Post-hoc comparisons confirmed that these reductions were specific to the rTMS group, with significantly decreased transition probabilities from A to C ($T(44) = 2.627$, $p = 0.012$, Cohen's $d = 0.392$) and from B to C ($T(44) = 2.895$, $p = 0.006$, Cohen's $d = 0.432$). No significant effects were found in the sham group (all $p > 0.058$) (Figure S6).

Long-term effects of OFC-rTMS on microstate dynamics in schizophrenia

Repeated-measures ANOVA comparing microstate parameters before and after the 20-day intervention revealed significant changes in microstate C and microstate D (Fig. 4). For microstate C, coverage showed a significant time × group interaction ($F(1, 85) = 4.246$, $p = 0.042$, $\eta^2_p = 0.044$), and occurrence showed a significant main effect of time ($F(1, 85) = 4.846$, $p = 0.030$, $\eta^2_p = 0.056$). Post hoc comparisons indicated that the rTMS group exhibited reduced coverage ($T(44) = 2.342$, $p = 0.024$, Cohen's $d = 0.349$) and occurrence ($T(44) = 2.189$, $p = 0.034$, Cohen's $d = 0.326$), while no significant changes were observed in the sham group (all $p > 0.490$). For microstate D, significant main effects of time were observed for duration ($F(1, 85) = 13.308$, $p < 0.001$, FDR-corrected $q = 0.011$, $\eta^2_p = 0.110$), coverage ($F(1, 85) = 12.596$, $p < 0.001$, FDR-corrected $q = 0.011$, $\eta^2_p = 0.109$), and occurrence ($F(1, 85) = 4.357$, $p = 0.040$, $\eta^2_p = 0.053$). Post hoc analyses showed that participants in the rTMS group exhibited significant increases in duration ($T(44) = 2.811$, $p = 0.007$, FDR-corrected $q = 0.037$, Cohen's $d = 0.385$), coverage ($T(44) = 3.535$, $p = 0.001$, FDR-corrected $q = 0.012$, Cohen's $d = 0.488$), and occurrence ($T(44) = 2.731$, $p = 0.009$, FDR-corrected $q = 0.037$, Cohen's $d = 0.407$). In the sham group, a significant increase was observed only for the duration of microstate D ($T(41) = 2.520$, $p = 0.016$, Cohen's $d = 0.352$).

State transition probability results are summarized in Figure S7. Significant time × group interactions were observed for transitions from microstate A to C ($F(1, 85) = 8.718$, $p = 0.004$, $\eta^2_p = 0.093$) and from B to C ($F(1, 85) = 6.394$, $p = 0.013$, $\eta^2_p = 0.072$). Post hoc analyses indicated reduced transition probabilities in the rTMS group from A to C ($T(44) = 2.942$, $p = 0.005$, FDR-corrected $q = 0.030$, Cohen's $d = 0.439$) and from B to C ($T(44) = 2.362$, $p = 0.023$, Cohen's $d = 0.352$), with no significant changes in the sham group. Additionally, transitions from microstates A and B to D showed significant main effects of time (A: $F(1, 85) = 8.357$, $p = 0.005$, FDR-corrected $q = 0.040$, $\eta^2_p = 0.082$; B: $F(1, 85) = 7.754$, $p = 0.007$, FDR-corrected $q = 0.042$, $\eta^2_p = 0.069$), as well as significant time × group interactions (A: $F(1, 85) = 6.619$, $p = 0.012$, $\eta^2_p = 0.076$; B: $F(1, 85) = 4.470$, $p = 0.037$, $\eta^2_p = 0.058$). A main effect of time was also found for the transition from C to D ($F(1, 85) = 6.424$, $p = 0.013$, $\eta^2_p = 0.057$). Follow-up comparisons showed increased transition probabilities in the rTMS group from A to D ($T(44) = 3.745$, $p < 0.001$, FDR-corrected $q = 0.002$, Cohen's $d = 0.558$), B to D ($T(44) = 3.141$, $p = 0.003$, FDR-corrected $q = 0.024$, Cohen's $d = 0.468$), and C to D ($T(44) = 2.787$, $p = 0.008$, FDR-corrected $q = 0.037$, Cohen's $d = 0.415$), while the sham group showed no significant changes (all $p > 0.256$).

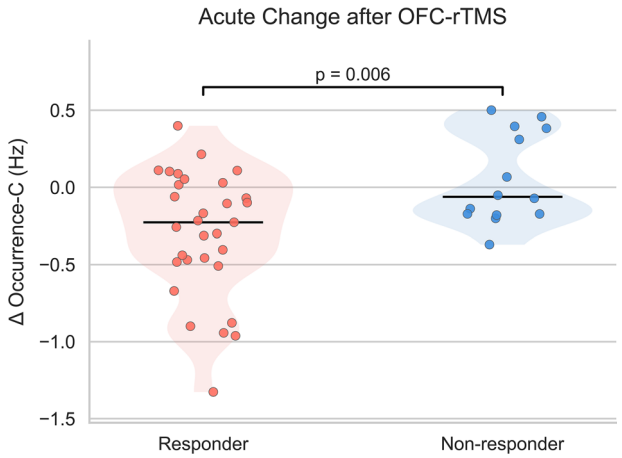

Fig. 5 Exploratory subgroup analysis of immediate changes following OFC-rTMS. Violin plot showing the immediate change (Δ Occurrence) of microstate C following a single OFC-rTMS session in responder and non-responder subgroups. Responders were defined as patients with ≥25% reduction in PANSS total scores after the 20-session intervention. A significant group difference was observed ($p = 0.006$). The black horizontal line indicate mean change in occurrence.

Relationship between immediate effects of single rTMS and treatment outcome

To explore whether immediate changes in brain dynamics following OFC-rTMS were associated with subsequent clinical improvement, an exploratory analysis was conducted within the rTMS group. Correlation analyses revealed no significant associations between changes in microstate parameters and reductions in PANSS total or subscale scores. To further examine potential predictive effects, participants were classified as responders ($N = 31$) or non-responders ($N = 14$) based on a ≥ 25% reduction in PANSS total scores after the 20-day intervention [32, 33]. Comparisons of immediate changes in microstate C occurrence revealed a significant difference between the two subgroups (responders: -0.295 ± 0.402; non-responders: 0.054 ± 0.294; $T(43) = 2.906$, $p = 0.006$, Cohen's $d = 0.936$; Fig. 5). At a significance level of 0.05, this sample size and observed effect corresponded to a statistical power of approximately 86%.

DISCUSSION

This study investigated how OFC-rTMS modulates abnormal EEG microstate dynamics in schizophrenia, focusing on both immediate and long-term effects. We first observed that a single session of 1 Hz stimulation acutely altered brain dynamics, evidenced by a reduction in the occurrence of microstate C in both patients and healthy controls. Longitudinal analyses further revealed that repeated stimulation over 20 sessions induced sustained changes, characterized by a persistent decrease in microstate C and a concurrent increase in microstate D across multiple temporal parameters. Notably, clinical responders to OFC-rTMS exhibited significantly greater immediate reductions in microstate C following the first session compared to non-responders. These findings suggest that EEG microstate changes may reflect neuromodulatory effects and hold promise as early biomarkers for predicting long-term OFC-rTMS treatment outcomes.

Our baseline analysis replicated prior reports showing elevated microstate C parameters in schizophrenia, reinforcing the view that alterations in microstate C are a core aspect of disrupted brain activity in this disorder [34, 35]. Gold et al. used EEG source localization to demonstrate that microstate C is primarily associated with activity in the dorsal anterior cingulate cortex (dACC), anterior insula (AI), and OFC, which are key regions within the salience network and the reward circuit [36]. These areas are critically involved in salience detection, reward evaluation, and the regulation of goal-directed behavior. Converging evidence from neuroimaging studies has shown that functional abnormalities in salience- and reward-related regions are common in schizophrenia [37, 38]. Such disruptions are thought to contribute to aberrant salience attribution, reduced motivation, and the emergence of core clinical symptoms such as delusions and anhedonia. Although microstate C appears to reflect these pathological mechanisms, previous studies have shown that antipsychotic medication does not reliably normalize its dynamics. No significant differences in microstate C parameters have been observed between medicated and unmedicated patients [39], nor before and after pharmacological treatment [40]. Similarly, interventions such as neurofeedback have failed to induce measurable changes in microstate C, suggesting limited efficacy in modulating the salience and reward systems [41]. Noninvasive neuromodulation may offer a promising alternative. Although some studies have reported changes in microstate C following high-frequency rTMS over the left DLPFC, these effects did not significantly differ from sham stimulation [26]. In contrast, the present results demonstrate that 1 Hz OFC-rTMS specifically reduced the temporal expression of microstate C—including decreases in coverage, occurrence, and transition probabilities from microstates A and B to C—relative to sham. This pattern suggests that inhibitory stimulation of the OFC may more effectively target the salience and reward systems. Moreover, our results show that microstate C decreased not only in patients but also in healthy controls following a single OFC stimulation session, indicating that the modulation of salient networks induced by OFC-rTMS is not specific to schizophrenia. Therefore, the observed change in microstate C may not represent a "pathological normalization" but rather a general, physiological modulation of core brain networks. This suggests that such network-level effects could be relevant across multiple disorders, which may help explain the reported efficacy of OFC-stimulation in depression, obsessive-compulsive disorder, and other affective conditions [9, 27, 42]. Neuroimaging studies in OCD support a similar mechanism, showing functional abnormalities in the dorsal anterior cingulate cortex (dACC), anterior insula (AI), and OFC [43, 44], and OFC-targeted stimulation has been reported to modulate these functional alterations [11, 45]. Together, these findings provide a rationale for applying OFC-rTMS in schizophrenia as a network-specific therapeutic strategy.

Beyond the long-term effects of OFC-rTMS, this study also examined the immediate impact of a single stimulation session on EEG microstate dynamics. Acute effects of a single rTMS session have been reported to persist for up to approximately one hour [46, 47]. Prior work has shown that single-session rTMS can acutely modulate microstate parameters, with the magnitude of change increasing with cumulative stimulation dose [48]. Differences in acute microstate responses have also been observed across stimulation targets, while sham stimulation consistently yields null effects [49, 50]. Consistent with these findings, we observed a significant reduction in the occurrence of microstate C immediately after a single OFC-rTMS session in both healthy controls and patients with schizophrenia. No comparable changes were found following sham stimulation, suggesting target-specific and stimulation-dependent modulation of brain dynamics. These findings indicate that even a single session of OFC stimulation is sufficient to induce measurable alterations in brain dynamics within regions associated with the salience network and reward circuitry. Importantly, exploratory subgroup analyses revealed that patients classified as responders, based on clinical improvement after the 20-session intervention, exhibited greater immediate reductions in microstate C occurrence following the first rTMS session compared to non-responders. Although the between-group difference at the 20-day post-intervention time point was

not statistically significant ($T(45) = 1.234$, $p = 0.225$, Cohen's $d = 0.396$), within-group analyses showed a significant reduction in microstate C occurrence for the responder group ($T(30) = 2.450$, $p = 0.020$, Cohen's $d = 0.440$), whereas the non-responder group did not exhibit a significant change ($T(13) = 0.221$, $p = 0.829$, Cohen's $d = 0.059$). These findings suggest that early changes in microstate C may serve as a potential biomarker of individual responsiveness to OFC-rTMS. Although baseline EEG features have been proposed as potential predictors of treatment outcomes [51], some studies have reported negative findings [24, 52]. In contrast to baseline measurements, brain changes assessed immediately after the first stimulation session may provide a more accurate and sensitive indicator of an individual's long-term neuromodulatory response and optimize personalized treatment planning. However, we did not identify significant associations between single-rTMS-induced microstate changes and clinical symptom improvement. Several factors may contribute to this finding. First, single-session neural effects may represent a "necessary but not sufficient" condition; that is, they could indicate potential responsiveness but do not linearly translate to long-term symptom improvement. Second, single-session effects might primarily reflect changes in specific symptom domains rather than the total PANSS score, which could weaken their apparent association with overall clinical improvement. Finally, the lack of significant correlations may be influenced by the limited sample size, highlighting the need for larger-scale clinical studies to more robustly examine the relationship between early neural responses and subsequent symptom changes.

In addition to effects on microstate C, the present findings revealed that long-term OFC-rTMS also modulated abnormal microstate D dynamics, including increases in duration, coverage, occurrence, and transition probabilities from microstates A, B, and C to D. Prior multimodal neuroimaging studies have linked microstate D to activity in regions associated with attentional control, particularly within right-lateralized dorsal and ventral frontoparietal networks [15, 53]. This configuration is thought to support the dynamic switching and reorientation of attention toward task-relevant stimuli [17]. Consistent with this interpretation, alterations in microstate D in schizophrenia have been associated with impairments in attentional allocation, context updating, and executive control [20, 54]. A previous study has suggested that reduced expression of microstate D is associated with the development of positive symptoms in schizophrenia [55]. Similarly, decreased microstate D has been observed during episodes of verbal hallucinations [56], suggesting a potential link between diminished microstate D activity and impaired error monitoring. In our study, significant changes in the temporal parameters of microstate D were observed in the rTMS group. However, a similar increase in microstate D duration was also noted in the sham group, and no significant differences were found between groups. Considering that antipsychotic medications primarily target positive symptoms [57], patients in our study were receiving pharmacological treatment, which may have contributed to the observed recovery of microstate D. This interpretation is supported by previous pharmacological research reporting increases in microstate D following antipsychotic treatment, particularly during periods of improvement in positive symptoms [22]. Although our correlation analyses did not reveal a significant association between changes in microstate D and improvements in positive symptoms (all $p > 0.138$), it remains plausible that the observed modulation of microstate D is not specific to OFC-rTMS but may instead reflect medication-related factors common to both groups. However, we cannot entirely rule out an effect of OFC-rTMS on microstate D, as the rTMS group exhibited a greater number of significant changes, despite the absence of between-group differences. While a single session of stimulation may be insufficient to elicit measurable cortical changes, repeated sessions could facilitate interactions between rTMS and concurrent pharmacotherapy. Specifically, concurrent antipsychotic treatment may alter cortical excitability, thereby modulating cortical plasticity and network dynamics, which could contribute to the delayed modulation of microstate D following rTMS [58].

Several limitations of this study should be acknowledged. First, multiple statistical comparisons were conducted across conditions and microstate parameters. While some findings survived FDR correction, others did not, and thus should be interpreted with caution and validated in future studies. Second, the present analysis focused exclusively on the temporal characteristics of microstates. Given the spatial variability of microstate topographies across individuals and groups, incorporating spatial features may provide additional insight into how OFC-rTMS modulates large-scale brain dynamics. Third, some patients received concurrent antipsychotic medication. Although baseline measures were balanced, medication may have confounded the findings because psychotropic drugs can affect cortical excitability and plasticity [59]. Future studies using rTMS alone are needed to clarify its specific effects on microstate dynamics. Finally, the sham procedure using a flipped coil may still generate a weak magnetic field and does not guarantee complete blinding. Future studies should adopt more effective sham designs and explicitly evaluate blinding success to enhance the rigor and validity of the findings.

In summary, this study investigated both the immediate and long-term effects of OFC-rTMS on EEG microstate dynamics. A single session of active stimulation led to a reduction in microstate C occurrence in both healthy controls and patients, whereas sham stimulation produced no significant changes. After 20 sessions, schizophrenia patients receiving active stimulation showed a selective decrease in microstate C and an increase in microstate D, reversing the pattern of abnormalities commonly observed in this population. Moreover, responder subgroup analysis indicated that greater acute reductions in microstate C were associated with better treatment outcomes, supporting the potential utility of early microstate changes as predictive biomarkers of OFC-rTMS efficacy.

DATA AVAILABILITY

The data used in this study are available from the corresponding author upon reasonable request.

CODE AVAILABILITY

The custom code used for data preprocessing, analysis, and visualization in this study is available from the corresponding author upon reasonable request.

REFERENCES

1. Collaborators GMD. Global, regional, and national burden of 12 mental disorders in 204 countries and territories, 1990-2019: a systematic analysis for the Global Burden of Disease Study 2019. Lancet Psychiatry. 2022;9:137–50.
2. Lally J, Gaughran F, Timms P, Curran SR. Treatment-resistant schizophrenia: current insights on the pharmacogenomics of antipsychotics. Pharmgenomics Pers Med. 2016;9:117–29.
3. Leucht S, Cipriani A, Spineli L, Mavridis D, Orey D, Richter F, et al. Comparative efficacy and tolerability of 15 antipsychotic drugs in schizophrenia: a multiple-treatments meta-analysis. Lancet. 2013;382:951–62.
4. Lefaucheur J-P, Aleman A, Baeken C, Benninger DH, Brunelin J, Di Lazzaro V, et al. Evidence-based guidelines on the therapeutic use of repetitive transcranial magnetic stimulation (rTMS): An update (2014-2018). Clin Neurophysiol. 2020;131:474–528.
5. Shi C, Yu X, Cheung EFC, Shum DHK, Chan RCK. Revisiting the therapeutic effect of rTMS on negative symptoms in schizophrenia: a meta-analysis. Psychiatry Res. 2014;215:505–13.
6. Blyth SH, Cruz Bosch C, Raffoul JJ, Chesley J, Johnson B, Borodge D, et al. Safety of rTMS for Schizophrenia: A Systematic Review and Meta-analysis. Schizophr Bull. 2025;51:392–400.

7. Fettes P, Schulze L, Downar J. Cortico-striatal-thalamic loop circuits of the orbitofrontal cortex: promising therapeutic targets in psychiatric illness. Front Syst Neurosci. 2017;11:25.
8. Prentice A, Kolken Y, Tuttle C, van Neijenhof J, Pitch R, van Oostrom I, et al. 1Hz right orbitofrontal TMS benefits depressed patients unresponsive to dorsolateral prefrontal cortex TMS. Brain Stimul. 2023;16:1572–5.
9. Feffer K, Fettes P, Giacobbe P, Daskalakis ZJ, Blumberger DM, Downar J. 1Hz rTMS of the right orbitofrontal cortex for major depression: Safety, tolerability and clinical outcomes. Eur Neuropsychopharmacol. 2018;28:109–17.
10. Grover S, Nguyen JA, Viswanathan V, Reinhart RMG. High-frequency neuromodulation improves obsessive-compulsive behavior. Nat Med. 2021;27:232–8.
11. Cheng J, Wang Y, Tang Y, Lin L, Gao J, Wang Z. EEG microstates are associated with the improvement of obsessive-compulsive symptoms after transcranial direct current stimulation. J Psychiatr Res. 2024;176:360–7.
12. Hu Q, Jiao X, Zhou J, Tang Y, Zhang T, Song C, et al. Low-frequency repetitive transcranial magnetic stimulation over the right orbitofrontal cortex for patients with first-episode schizophrenia: a randomized, double-blind, sham-controlled trial. Psychiatry Res. 2023;330:115600.
13. Jiao X, Hu Q, Tang Y, Zhang T, Zhang J, Wang X, et al. Abnormal global cortical responses in drug-naïve patients with schizophrenia following orbitofrontal cortex stimulation: a concurrent transcranial magnetic stimulation-electroencephalography study. Biol Psychiatry. 2024;96:342–51.
14. Zhang K, Shi W, Wang C, Li Y, Liu Z, Liu T, et al. Reliability of EEG microstate analysis at different electrode densities during propofol-induced transitions of brain states. Neuroimage. 2021;231:117861.
15. Musso F, Brinkmeyer J, Mobascher A, Warbrick T, Winterer G. Spontaneous brain activity and EEG microstates. A novel EEG/fMRI analysis approach to explore resting-state networks. Neuroimage. 2010;52:1149–61.
16. Michel CM, Koenig T. EEG microstates as a tool for studying the temporal dynamics of whole-brain neuronal networks: A review. Neuroimage. 2018;180:577–93.
17. Britz J, Van De Ville D, Michel CM. BOLD correlates of EEG topography reveal rapid resting-state network dynamics. Neuroimage. 2010;52:1162–70.
18. da Cruz JR, Favrod O, Roinishvili M, Chkonia E, Brand A, Mohr C, et al. EEG microstates are a candidate endophenotype for schizophrenia. Nat Commun. 2020;11:3089.
19. Rieger K, Diaz Hernandez L, Baenninger A, Koenig T. 15 Years of Microstate Research in Schizophrenia - Where Are We? A Meta-Analysis. Front Psychiatry. 2016;7:22.
20. Iftimovici A, Marchi A, Férat V, Pruvost-Robieux E, Guinard E, Morin V, et al. Electroencephalography microstates imbalance across the spectrum of early psychosis, autism, and mood disorders. Eur Psychiatry. 2023;66:e41.
21. Sun Q, Zhou J, Guo H, Gou N, Lin R, Huang Y, et al. EEG microstates and its relationship with clinical symptoms in patients with schizophrenia. Front Psychiatry. 2021;12:761203.
22. de Bock R, Mackintosh AJ, Maier F, Borgwardt S, Riecher-Rössler A, Andreou C. EEG microstates as biomarker for psychosis in ultra-high-risk patients. Transl Psychiatry. 2020;10:300.
23. Liu Z, Wu S, Wang S, Wu H, Gao H, Lu X. Can repetitive transcranial magnetic stimulation promote recovery of consciousness in patients with disorders of consciousness? A randomized controlled trial. Neuroimage Clin. 2025;46:103802.
24. Gold MC, Yuan S, Tirrell E, Kronenberg EF, Kang JWD, Hindley L, et al. Large-scale EEG neural network changes in response to therapeutic TMS. Brain Stimul. 2022;15:316–25.
25. Ding X, Li X, Xu M, He Z, Jiang H. The effect of repetitive transcranial magnetic stimulation on electroencephalography microstates of patients with heroin-addiction. Psychiatry Res Neuroimaging. 2023;329:111594.
26. Liu S, Yang S, Feng K, Wang C, Wang L. A study on the effects of repetitive transcranial magnetic stimulation on EEG microstate in patients with Parkinson's disease. IEEE Trans Neural Syst Rehabil Eng. 2024;32:3369–77.
27. Khedr EM, Elbeh K, Saber M, Abdelrady Z, Abdelwarith A. A double blind randomized clinical trial of the effectiveness of low frequency rTMS over right DLPFC or OFC for treatment of obsessive-compulsive disorder. J Psychiatr Res. 2022;156:122–31.
28. Delorme A, Makeig S. EEGLAB: an open source toolbox for analysis of single-trial EEG dynamics including independent component analysis. J Neurosci Methods. 2004;134:9–21.
29. Murray MM, Brunet D, Michel CM. Topographic ERP analyses: a step-by-step tutorial review. Brain Topogr. 2008;20:249–64.
30. Pascual-Marqui RD, Michel CM, Lehmann D. Segmentation of brain electrical activity into microstates: model estimation and validation. IEEE Trans Biomed Eng. 1995;42:658–65.
31. Liu J, Xu J, Zou G, He Y, Zou Q, Gao J-H. Reliability and individual specificity of EEG microstate characteristics. Brain Topography. 2020;33:438–49.
32. Correll CU, Kishimoto T, Nielsen J, Kane JM. Quantifying clinical relevance in the treatment of schizophrenia. Clinical Therapeutics. 2011;33:B16–B39.
33. Leucht S, Davis J, Engel R, Kissling W, Kane J. Definitions of response and remission in schizophrenia: recommendations for their use and their presentation. Acta Psychiatrica Scandinavica. 2009;119:7–14.
34. Kim K, Duc NT, Choi M, Lee B. EEG microstate features for schizophrenia classification. PLoS One. 2021;16:e0251842.
35. Thirioux B, Langbour N, Bokam P, Wassouf I, Guillard-Bouhet N, Wangermez C, et al. EEG microstate co-specificity in schizophrenia and obsessive-compulsive disorder. Eur Arch Psychiatry Clin Neurosci. 2024;274:207–25.
36. Nishida K, Morishima Y, Yoshimura M, Isotani T, Irisawa S, Jann K, et al. EEG microstates associated with salience and frontoparietal networks in frontotemporal dementia, schizophrenia and Alzheimer's disease. Clin Neurophysiol. 2013;124:1106–14.
37. Gradin VB, Waiter G, O'Connor A, Romaniuk L, Stickle C, Matthews K, et al. Salience network-midbrain dysconnectivity and blunted reward signals in schizophrenia. Psychiatry Res. 2013;211:104–11.
38. Nudelman JL, Waltz JA. Acute and lifetime stress and psychotic illness: the roles of reward and salience networks. J Psychiatr Brain Sci. 2022;7:e220012.
39. Mackintosh AJ, Borgwardt S, Studerus E, Riecher-Rössler A, de Bock R, Andreou C. EEG microstate differences in medicated vs. medication-naïve first-episode psychosis patients. Front Psychiatry. 2020;11:600606.
40. Kikuchi M, Koenig T, Wada Y, Higashima M, Koshino Y, Strik W, et al. Native EEG and treatment effects in neuroleptic-naïve schizophrenic patients: time and frequency domain approaches. Schizophr Res. 2007;97:163–72.
41. Diaz Hernandez L, Rieger K, Baenninger A, Brandeis D, Koenig T. Towards using microstate-neurofeedback for the treatment of psychotic symptoms in schizophrenia. A feasibility study in healthy participants. Brain Topogr. 2016;29:308–21.
42. Rao VR, Sellers KK, Wallace DL, Lee MB, Bijanzadeh M, Sani OG, et al. Direct electrical stimulation of lateral orbitofrontal cortex acutely improves mood in individuals with symptoms of depression. Curr Biol. 2018;28:3893–902. e3894.
43. Fan J, Zhong M, Zhu X, Gan J, Liu W, Niu C, et al. Resting-state functional connectivity between right anterior insula and right orbital frontal cortex correlate with insight level in obsessive-compulsive disorder. Neuroimage Clin. 2017;15:1–7.
44. Hou J, Wu W, Lin Y, Wang J, Zhou D, Guo J, et al. Localization of cerebral functional deficits in patients with obsessive-compulsive disorder: a resting-state fMRI study. J Affect Disord. 2012;138:313–21.
45. Nauczyciel C, Le Jeune F, Naudet F, Douabin S, Esquevin A, Vérin M, et al. Repetitive transcranial magnetic stimulation over the orbitofrontal cortex for obsessive-compulsive disorder: a double-blind, crossover study. Transl Psychiatry. 2014;4:e436.
46. Thut G, Pascual-Leone A. A review of combined TMS-EEG studies to characterize lasting effects of repetitive TMS and assess their usefulness in cognitive and clinical neuroscience. Brain Topography. 2009;22:219–32.
47. Qiu S, Wang S, Yi W, Zhang C, He H. The lasting effects of 1Hz repetitive transcranial magnetic stimulation on resting state EEG in healthy subjects. Annu Int Conf IEEE Eng Med Biol Soc. 2019;2019:5918–22.
48. Qiu S, Wang S, Yi W, Zhang C, He H. Changes of resting-state EEG microstates induced by low-frequency repetitive transcranial magnetic stimulation. Annu Int Conf IEEE Eng Med Biol Soc. 2020;2020:3549–52.
49. Croce P, Zappasodi F, Capotosto P. Offline stimulation of human parietal cortex differently affects resting EEG microstates. Sci Rep. 2018;8:1287.
50. Croce P, Spadone S, Zappasodi F, Baldassarre A, Capotosto P. rTMS affects EEG microstates dynamic during evoked activity. Cortex. 2021;138:302–10.
51. Guo Y, Zhao X, Liu X, Liu J, Li Y, Yue L, et al. Electroencephalography microstates as novel functional biomarkers for insomnia disorder. Gen Psychiatr. 2023;36:e101171.
52. Zhdanov A, Atluri S, Wong W, Vaghei Y, Daskalakis ZJ, Blumberger DM, et al. Use of machine learning for predicting escitalopram treatment outcome from electroencephalography recordings in adult patients with depression. JAMA Netw Open. 2020;3:e1918377.
53. Atluri S, Wong W, Moreno S, Blumberger DM, Daskalakis ZJ, Farzan F. Selective modulation of brain network dynamics by seizure therapy in treatment-resistant depression. Neuroimage Clin. 2018;20:1176–90.
54. Yao R, Song M, Shi L, Pei Y, Li H, Tan S, et al. Microstate D as a biomarker in schizophrenia: insights from brain state transitions. Brain Sci. 2024;14:985.
55. Koenig T, Lehmann D, Merlo MC, Kochi K, Hell D, Koukkou M. A deviant EEG brain microstate in acute, neuroleptic-naive schizophrenics at rest. Eur Arch Psychiatry Clin Neurosci. 1999;249:205–11.
56. Kindler J, Hubl D, Strik WK, Dierks T, Koenig T. Resting-state EEG in schizophrenia: auditory verbal hallucinations are related to shortening of specific microstates. Clin Neurophysiol. 2011;122:1179–82.

57. Amato D, Vernon AC, Papaleo F. Dopamine, the antipsychotic molecule: a perspective on mechanisms underlying antipsychotic response variability. Neurosci Biobehav Rev. 2018;85:146–59.
58. Sohn MN, Brown JC, Sharma P, Ziemann U, McGirr A. Pharmacological adjuncts and transcranial magnetic stimulation-induced synaptic plasticity: a systematic review. J Psychiatry Neurosci. 2024;49:E59–E76.
59. Minzenberg M, Leuchter A. The effect of psychotropic drugs on cortical excitability and plasticity measured with transcranial magnetic stimulation: Implications for psychiatric treatment. J Affect Disord. 2019;253:126–40.

AUTHOR CONTRIBUTIONS

Kexu Zhang: Conceptualization, Formal analysis, Methodology, Software, Visualization, Writing – review & editing, Writing – original draft. Xiong Jiao: Data curation, Project administration, Writing – review & editing, Writing – original draft. Yanli Zhang: Data curation, Validation, Visualization. Ningning Zeng: Software, Methodology. Min Wang: Data curation, Validation. Kun Li: Resources, Supervision, Writing – review & editing. Ziliang Wang: Data curation, Funding acquisition, Investigation. Chunbo Li: Project administration, Writing – review & editing. Jijun Wang: Supervision, Funding acquisition, Writing – review & editing. Qiang Hu: Data curation, Funding acquisition, Writing – review & editing, Writing – original draft.

FUNDING

This work was supported by the National Natural Science Foundation of China (Grant No. 82151314), the Clinical Research Plan of Shanghai Hospital Development Center (Grant No. SHDC12022113), the Shanghai Municipal Health Commission (Grant No. 20254Y0117), the Zhenjiang Science and Technology Plan Projects (Grant Nos. SH2024013, SH2024018, JC2024042, JC2024043), the Jiangsu Natural Science Foundation Youth Project (Grant No. BK20240506), the Research Foundation of the Jiangsu Provincial Commission of Health and Family Planning (Grant Nos. H2023036, H2024099), and the Jiangsu Provincial Administration of Traditional Chinese Medicine Project (Grant No. MS2024122). The authors gratefully acknowledge their support.

COMPETING INTERESTS

The authors declare no competing interests.

ADDITIONAL INFORMATION

Supplementary information The online version contains supplementary material available at https://doi.org/10.1038/s41398-026-03810-3.

Correspondence and requests for materials should be addressed to Junfeng Sun, Jijun Wang or Xiong Jiao.